WILEY InterScience® DISCOVER SOMETHING GREAT

PROTEINS STRUCTURE ■ FUNCTION ■ BIOINFORMATICS

Common conformational changes in flavodoxins induced by FMN and anion binding: The structure of *Helicobacter pylori* apoflavodoxin

Marta Martínez-Júlvez,[1,2] Nunilo Cremades,[1,2] Marta Bueno,[1,2] Inmaculada Pérez-Dorado,[3] Celia Maya,[3] Santiago Cuesta-López,[1,4] Diego Prada,[1,4] Fernando Falo,[1,4] Juan A. Hermoso,[3]* and Javier Sancho[1,2]*

[1] Biocomputation and Complex Systems Physics Institute (BiFi), Universidad de Zaragoza, Unidad Asociada al IQFR-CSIC

[2] Departamento de Bioquímica y Biología Molecular y Celular, Facultad de Ciencias, Universidad de Zaragoza, 50009 Zaragoza, Spain

[3] Grupo de Cristalografía Molecular y Biología Estructural, Instituto Química-Física Rocasolano, Consejo Superior de Investigaciones Científicas, Serrano 119, 28006 Madrid, Spain

[4] Departamento de Física de la Materia Condensada, Facultad de Ciencias, Universidad de Zaragoza

ABSTRACT

Flavodoxins, noncovalent complexes between apoflavodoxins and flavin mononucleotide (FMN), are useful models to investigate the mechanism of protein/flavin recognition. In this respect, the only available crystal structure of an apoflavodoxin (that from* Anabaena*) showed a closed isoalloxazine pocket and the presence of a bound phosphate ion, which posed many questions on the recognition mechanism and on the potential physiological role exerted by phosphate ions. To address these issues we report here the X-ray structure of the apoflavodoxin from the pathogen* Helicobacter pylori*. The protein naturally lacks one of the conserved aromatic residues that close the isoalloxazine pocket in* Anabaena*, and the structure has been determined in a medium lacking phosphate. In spite of these significant differences, the isoallozaxine pocket in* H. pylori *apoflavodoxin appears also closed and a chloride ion is bound at a native-like FMN phosphate site. It seems thus that it is a general characteristic of apoflavodoxins to display closed, non-native, isoalloxazine binding sites together with native-like, rather promiscuous, phosphate binding sites that can bear other available small anions present in solution. In this respect, both binding energy hot spots of the apoflavodoxin/FMN complex are initially unavailable to FMN binding and the specific spot for FMN recognition may depend on the dynamics of the two candidate regions. Molecular dynamics simulations show that the isoalloxazine binding loops are intrinsically flexible at physiological temperatures, thus facilitating the intercalation of the cofactor, and that their mobility is modulated by the anion bound at the phosphate site.

Proteins 2007; 69:581–594.

Key words: ligand binding; chloride; Helicobacter pylori*; protein stability; molecular recognition.*

INTRODUCTION

Many proteins are noncovalent, spontaneously assembled complexes between a polypeptide moiety, the apoprotein, and a small ligand, that is: a metal ion or a small organic molecule, that recognize one another. Understanding protein/ligand recognition is one of the challenges in Structural Biology and bears on many important fields such as protein folding, drug design, and catalysis. Among the proteins carrying noncovalently bound cofactors, flavodoxins have attracted much interest.[1–3] They are electron transfer proteins and contain one molecule of flavin nucleotide (FMN). Their relatively small size (between 14 and 18 kDa), ease of purification, and reversibility towards FMN removal, together with the early availability of the X-ray structures of several flavodoxins[4,5] have made them widely used to investigate protein–protein electron transfer,[6–8] the kinetics and thermodynamics of protein ligand recognition,[9,10] and protein folding, and stability issues.[11–17] Recently, flavodoxins from several pathogenic organisms have been identified as essential for their survival[18,19] and it has been pointed out that those flavodoxins could be used as targets for drug design.[19,20]

Grant sponsor: Ministerio de Educación y Ciencia (Spain); Grant numbers: BFU2004-01411, PM076/2006; Grant sponsor: Spanish Ministry of Education; Grant number: FIS2005-00337.
*Correspondence to: Juan. A. Hermoso, Grupo de Cristalografía Molecular y Biología Estructural, Instituto Química-Física Rocasolano, Consejo Superior de Investigaciones Científicas, Serrano 119, 28006 Madrid, Spain. E-mail: xjuan@iqfr.csic.es or Javier Sancho, Biocomputation and Complex Systems Physics Institute (BiFi), Universidad de Zaragoza, Unidad Asociada al IQFR-CSIC or Departamento de Bioquímica y Biología Molecular y Celular, Facultad de Ciencias, Universidad de Zaragoza, 50009 Zaragoza, Spain. E-mail: jsancho@unizar.es
Received 15 June 2006; Revised 15 November 2006; Accepted 16 December 2006
Published online 10 July 2007 in Wiley InterScience (www.interscience.wiley.com).
DOI: 10.1002/prot.21410

One difficulty to investigate the apoflavodoxin/FMN interaction is that, while many structures of the functional complexes are available,[2,19,21–25] it has been difficult to experimentally obtain three-dimensional structures of apoflavodoxins. NMR studies on *A. vinelandii*[26] and *Anabaena* PCC 7119[27] have provided valuable information, suggestive of conformational flexibility at the FMN binding site, but have not produced an apoflavodoxin structure yet. The only apoflavodoxin structure available until now is that of *Anabaena* PCC 7119 that was solved by X-ray diffraction using ammonium sulphate as precipitant.[28] The structure indicates that the overall fold of the protein is already present in the apo form, which is consistent with the spectroscopic and thermodynamic information.[13–27] When compared with the X-ray structure of its corresponding holo form,[24] the more significant differences are confined to one of the three short loops involved in FMN recognition: the loop bearing a conserved tryptophan residue (Trp57), that packs against the protruding methyl groups of FMN in most flavodoxins. In contrast, the loop containing Tyr94, a most conserved residue in flavodoxins that lies parallel on the isoalloxazine ring of FMN, is hardly affected. As for the third binding loop, the one extending from the N-terminus of helix 1 and providing hydrogen bonding groups for the FMN phosphate, its conformation is almost identical to that observed in the functional holoflavodoxin complex and, in fact, a sulphate or a phosphate ion is found in the crystal mimicking the FMN phosphate of the holoprotein (see Fig. 2 in Ref. 28). In the apoflavodoxin structure, a conformational change in the Trp loop brings this residue into contact with the side chain of Tyr94 so that an aromatic/aromatic interaction is formed that closes the isoalloxazine binding site. The high ionic strength of the buffer used to crystallise the protein could strengthen such interaction. Based on the native conformation of the phosphate binding site observed in the *Anabaena* apoflavodoxin structure, and on the closure of the isoalloxazine binding site, it was proposed that the binding of the FMN molecule to apoflavodoxin could start by interaction of the phosphate at the preformed binding site and then the interacting aromatic residues at the isoalloxazine site would open apart so that the FMN would finally achieve its functional conformation within the complex.[28] However, a mutational study of the transition state of complex formation[10] has shown that FMN first binds to apoflavodoxin by interaction of the isoalloxazine with the two aromatic residues, chiefly with Tyr 94, and that the interaction at the phosphate binding site takes place after the rate limiting step.

Whether the reported X-ray structure of *Anabaena* apoflavodoxin reflects faithfully the conformation of the protein in solution is not clear. The observed closure of the FMN binding site could be a consequence of the interaction between the two aromatic residues, which could be driven by the high ionic strength conditions, and the native-like conformation of the phosphate binding site could be induced by the high concentration of sulphate in the crystallization buffer, as noted in the original work.[28] In fact, the available NMR evidence on both the *Anabaena* and *Azotobacter* apoflavodoxins suggest that the binding site loops could be more flexible than seen in the X-ray structure.[26,27]

To address these issues, the X-ray structure of apoflavodoxin from the pathogen *Helicobacter pylori* has been solved. Although it shares significant sequence identity with the apoflavodoxin from *Anabaena* (43%), the *Helicobacter* protein lacks an FMN-binding Trp residue, and bears an Ala residue at the structurally equivalent position.[19] Care has been taken so that the crystallisation conditions were of a much lower ionic strength and that no sulphate or phosphate ions were present in the solution. Interestingly, and in spite of the differences in protein sequence and in crystallization conditions, the *H. pylori* apoflavodoxin also shows a closed isoalloxazine binding site and a well-folded phosphate binding site where a chloride ion appears bound. The implications of these findings for the mechanism of FMN recognition by apoflavodoxin and the potential role of anions bound at the phosphate site on the dynamics of the binding loops will be discussed.

MATERIALS AND METHODS

Recombinant expression of flavodoxin from *H. pylori*

DNA isolation and PCR amplification of the *fldA* gene have been reported.[20] Shortly, the flavodoxin gene *fldA* was amplified by PCR from total genomic *Helicobacter pylori* DNA (isolated form antigen-positive stool samples). The amplified sequence was gel-purified and cloned into pET28a (*Novagen*) using standard techniques. The translated protein sequence (the gene product of *H. pylori* cells isolated from a patient) shows four differences (S44, E124, S153, and K160) with that of the holoprotein (G44, A124, A153, and R160) whose X-ray structure has been reported[19] and that corresponds to *H. pylori* strain 69A. The four positions are solvent exposed and the residues involved are not related to FMN binding.

E. coli BL21 cells containing the pET28a-fldA plasmid were grown in Luria-Bertani medium containing 20 μg/mL of kanamycine and flavodoxin expression was induced with 1 m*M* isopropyl β-D-thiogalactoside. Flavodoxin was purified by precipitating bulk proteins in 65% ammonium sulphate, loading the supernatant in a DE-52 DEAE-cellulose column, eluting the protein with a reverse linear gradient of $(NH_4)_2SO_4$ (from 65 to 0%) and finally performing an additional DE-52 DEAE-cellulose chromatography, in the absence of ammonium sulphate, eluting with a linear NaCl gradient (from 0 to 0.5 *M*).[20] The recovered holoprotein was pure according to SDS-PAGE and to the ratio of its UV and visible absorbances.

DOI 10.1002/prot

Preparation and quantitation of apoflavodoxin

The flavin mononucleotide group was removed from the purified holoprotein by several cycles of apoprotein precipitation in 3% trichloroacetic acid.[29] In each cycle, the supernatant is removed and the pellet resuspended in 3% trichloroacetic acid. The FMN is considered to be removed when the supernatant is colorless and the pellet, dissolved in an appropriate buffer, shows no absorbance in the visible region. The concentration of the apoflavodoxin samples in the crystallization trials was calculated using an extinction coefficient of 15.9 mM^{-1} cm^{-1} at 280 nm determined in MOPS 50 m*M*, pH 7.0.[30]

Crystal growth, data collection, and structure refinement

The initial crystallization screening was done using a grid of PEG4K (28–32%) at different pHs (from 6.5 to 9.0) and 0.2 *M* $MgCl_2$. The condition containing 30% PEG 4K, 0.1 *M* HEPES/Na, pH 7.5 and 0.2 $MgCl_2$ mixed in 1:1 ratio with a 5 mg mL^{-1} protein solution produced some crystals, not good enough, that were improved using additive Screens I, II, and III from *Hampton*. Additive 20 from Screen I (benzamidine) was selected. Crystals of the apoflavodoxin from *Helicobacter pylori* where thus obtained by the hanging drop method, using droplets of 5 μL containing 2.25 μL of 5 mg mL^{-1} of protein solution buffered with 10 m*M* MOPS, pH 7.0, 2.25 μL of reservoir solution containing 30% PEG 4K, 0.1 *M* HEPES/Na, pH 7.5, 0.2 *M* $MgCl_2$ and 0.5 μL of 0.1 *M* benzamidine. Drops were equilibrated against 1 mL of reservoir solution at 4°C. The crystals grew within 1–7 days up to a maximum size of 0.1 × 0.1 × 0.2 mm^3. A single crystal was mounted in a cryoloop of 0.2 mm diameter. The cryobuffer consisted in the mother liquid supplemented with 20% glycerol. The diffraction data were collected at 120 K on a CCD detector using graphite-monochromated CuK_α radiation generated by a Bruker-Nonius rotating anode generator. The crystals belong to the $P2_12_12_1$ orthorhombic space group with unit cell dimensions of $a = 36.61$ Å, $b = 45.71$ Å, and $c = 86.65$ Å. The V_M is 2.13 $Å^3$/Da with one protein molecule in the asymmetric unit and 42.3% of solvent content. Collected data with a resolution limit of 2.1 Å were reduced with Denzo/Scalepack.[31]

The structure of apoflavodoxin was solved by molecular replacement using the program MOLREP[32] and taking as a model the structure of oxidized *H. pylori* holoflavodoxin[19] (PDB code 1FUE). A correlation of 0.52 was obtained, with an R-factor of 0.44. The generated single solution for the rotation and translation functions was refined with REFMAC 5.0.[33] The model was subjected to rigid body refinement and the coordinate parameters were minimized to satisfy Maximum Likelihood. This process was alternated with manual model building with the software package O.[34] Crystallographic data and statistics of the model are summarized in Table I. The final model contains 163 residues, one chloride anion, one benzamidine molecule, and 111 water molecules. The B-factors of the chloride anion and coordinating residues are Cl: 8.55, Thr10 (OG1): 12.34, Ser12 (OG): 19.85 and Ala15 (N): 14.11. The final values for *R* and R_{free} factors were 0.20 and 0.28, respectively. All residues in the Ramachandran plot fall within the allowed regions.

Table I
Data Collection and Refinement Statistics for Helicobacter pylori *Apoflavodoxin*[a]

Data collection statistics	
Space group	$P2_12_12_1$
Unit cell parameters	
a (Å)	36.61
b (Å)	45.71
c (Å)	86.65
Wavelength (Å)	1.5418
Resolution (Å)	20.3–2.1
No. of unique reflections	9402
Redundancy	5.1 (1.8)
Completeness (%)	98.9 (90.4)
I/σ	11.8 (1.3)
R_{sym}[b]	0.17 (0.56)
Refinement statistics	
Resolution range, Å	20.3–2.1
Protein nonhydrogen atoms	1228
Ligand nonhydrogen atoms	10
Solvent nonhydrogen atoms	111
R_{work}	0.20
R_{free}[c]	0.28
rmsd bond length (Å)	0.014
rmsd bond angles (°)	1.464
Average B-factor ($Å^2$)	19.55

[a]Values in parentheses correspond to the highest resolution shell.
[b]$R_{sym} = \Sigma|I - I_{av}|/\Sigma I$, where the summation is over symmetry equivalent reflections.
[c]*R* calculated for 7% of data excluded from the refinement.

Normal mode calculation and molecular dynamics simulations

Normal mode calculations[35] at atomic resolution were performed using the Vibran module and Hessian diagonalization routines implemented in the CHARMM program and c27b2 force field.[36,37] Initially, the protein was analyzed *in vaccuo* using extended electrostatics with no cut-offs criteria. To get insight into the minima landscape, different exploration routines were used combining steepest descent steps with adopted basis Newton Raphson, beginning with some harmonic constraints to leave at the end the system free. Chloride effects in the structure where introduced in two ways. Implicitly, via an increment in the rigidity of the neighboring residues, through soft harmonic mass constraints (typically 0.1–1 kcal mol^{-1} $Å^{-2}$), or explicitly, introducing the chloride atom with a soft positional constraint in order to avoid further diffusion from the specific site.

Normal modes analysis (NMA) at a coarse-grained scale was performed using the method developed by Tirion,[38] based on the so-called Gaussian Network Model (GNM)[39] and widely used in recent years.[40–42] After reaching a minimum energy configuration a contact map was calculated by considering the distance between C_α atoms, so that the atoms of any C_α pair with a distance below a given cutoff (R_c) were linked by a harmonic force building an elastic network. A cut-off criterion of 10 Å was chosen by fitting the experimental B-factors to the theoretical calculation. Normal modes and correlations of fluctuations can be obtained from eigenvalues and eigenvectors of this contact matrix.[39]

$$B_i^{\mathrm{GNM}} = 8\pi^2\langle \Delta R_i \cdot \Delta R_j \rangle/3 = (8\pi^2 K_B T/3\gamma)\Gamma_{i,j}^{-1}$$

This calculation is less time consuming than the all-atom approach (see below) and provides useful information on the backbone mobility of the protein, the elasticity properties, and how the movement of different regions are correlated. The effect of the chloride ion has been implemented in a similar way to that described above using a harmonic constraint to the position of residues linked to the ion.

On the other hand, molecular dynamics trajectories were generated using Langevin dynamics and implicit solvent with a friction coefficient[43] of 10–30 ps^{-1} and Eef1,[31] a force field with implicit solvation implemented in CHARMM. Trajectories were generated at different temperatures ranging from 50 to 330 K, in order to explore the temperature dependence of the behavior of critical structural regions of the protein. The production phase for each trajectory was of 10 ns, and began after a deep minimization of the crystal structure followed by a pre-equilibration run of 1 ns. Analysis of the trajectories and low frequency modes involving residues related to FMN binding, were done using principal component analysis (PCA)[44,45] along the last stable 4 ns of each run, coupling the Quasiharmonics routine implemented in CHARMM to a set of home made programs.

Binding assays

The dissociation constant of the holoflavodoxin-benzamidine complex was determined by titration of FMN emission fluorescence (excitation at 464 nm, and emission at 525 nm) in an *Aminco-Bowman Series 2* Spectrometer at (25 ± 0.1)°C (in darkness). Protein samples were prepared by mixing 900-μL ligand solutions of different concentrations with 100-μL aliquots of 40 μ*M* holoprotein, in 10 m*M* sodium phosphate, pH 7.0 and were allowed to equilibrate for 14 h. The dissociation constants were calculated by fitting the emission fluorescence data, as previously described.[20]

RESULTS AND DISCUSSION

Structure of *H. pylori* apoflavodoxin: conformational changes at the FMN binding site

The structure of the apoflavodoxin from *H. pylori* has been solved at 2.1 Å resolution. The protein displays the typical α/β-fold of the family [Fig. 1(A)]. The apoflavodoxin model contains also one chloride anion whose binding mimics that of the FMN phosphate in the holoprotein, one molecule of benzamidine (a crystallisation additive) bound far away from the FMN binding loops, and 111 water molecules.

The apo and holo forms are globally very similar (rmsd of 0.53 Å for all C_α atoms) [see Fig. 1(B)], indicating that the native folding of the protein is already achieved in the absence of the FMN cofactor. Significant differences between the structures of the apo and holo forms are concentrated in the FMN binding-site and in strand β5. This strand appears typically split in long-chain flavodoxins by an insertion of about 20 residues whose role in protein structure, stability, and function has been recently investigated.[46,47] The highest deviation in this region between the apo and holo flavodoxins corresponds to Gly131 (rmsd of 1.1 Å). In the FMN-binding site, deviations are concentrated in the regions that bind the isoalloxazine ring and the phosphate group of FMN [Fig. 1(C)]. The largest deviation is located in the 55–57 isoalloxazine binding loop, where flavodoxins usually display a tryptophan residue that in the *H. pylori* protein is replaced by an alanine. Large changes in the dihedral angles of residues 55–57 take place upon FMN binding [Fig. 1(B)] so that the rms deviation of all atoms of the 55–57 tripeptide in the apo and holo structures is 1.87 Å and that of Gly56 2.60 Å. The second largest deviation between the two structures is observed for residues 94–95 (rmsd of 0.96 Å), located in the additional loop involved in isoalloxazine binding (loop 88–98). This loop bears a conserved tyrosine residue (Tyr92) that packs against the *re*-face of the FMN ring in *H. pylori* holoflavodoxin. The changes in the dihedral angles of residues 94 and 95 are much smaller than those observed for the 55–60 loop but enough to allow the Tyr92 side chain to get closer and contact Gly56. The distance between the Gly56 carbonyl oxygen and the CZ atom of Tyr92 is of just 3.23 Å in apoflavodoxin, compared to 8.20 Å in the holoprotein. A concerted conformational change thus approximates the Tyr92 side chain and the 55–57 residues of the adjacent loop so that the space left by the missing FMN is partly filled. The rest of the cavity contains three ordered water molecules at positions close to those of the O2, N10, and O4 FMN atoms and one with coordinates intermediate between those of the CM7 and CM8 FMN atoms [Fig. 1(C)]. These solvent molecules are hydrogen bonded to protein residues and seem to contribute to the stability of the binding pocket. The water molecule

DOI 10.1002/prot

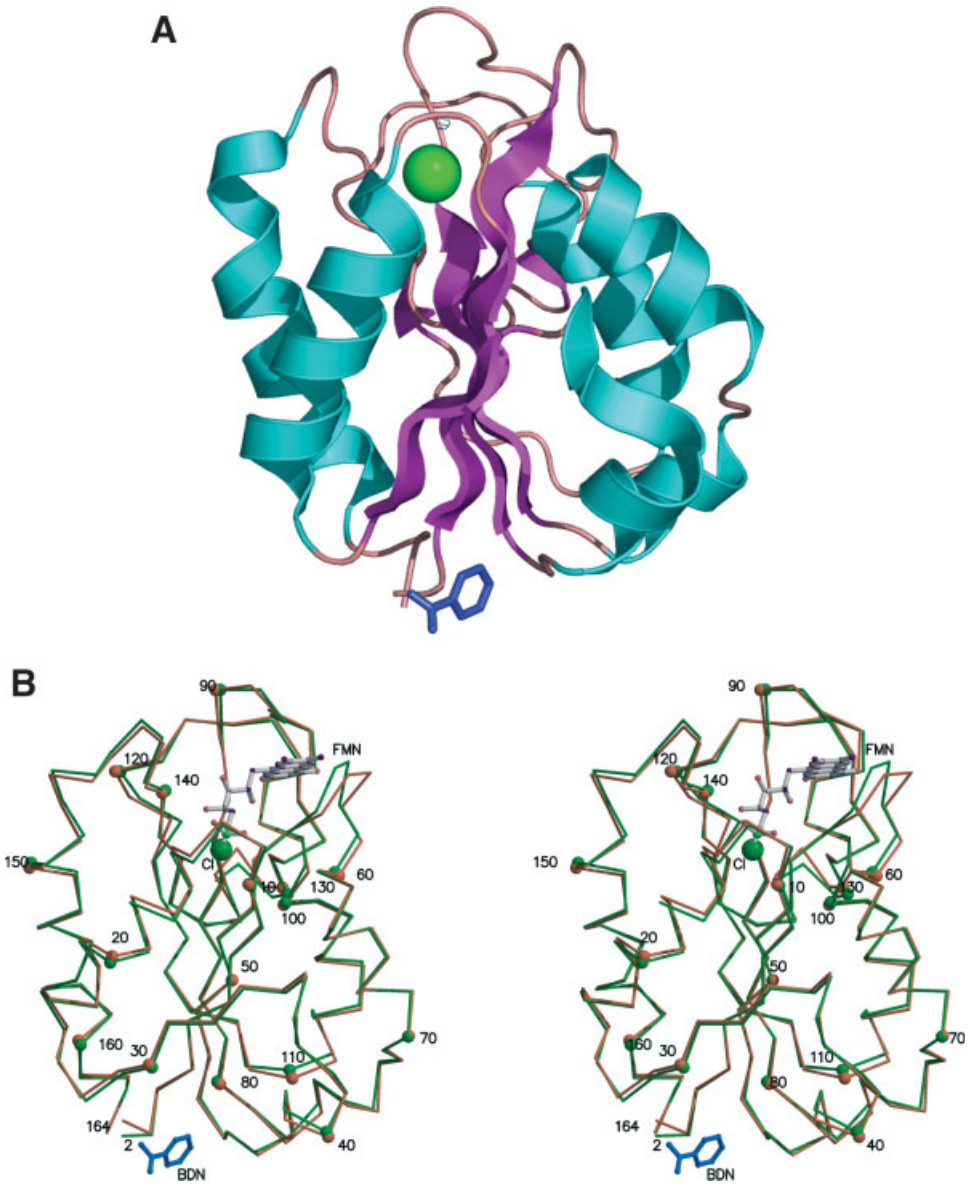

Figure 1

*(**A**) Ribbon diagram of* H. pylori *apoflavodoxin. The bound chloride is represented as a green sphere and the benzamidine molecule as blue sticks. (**B**) Stereo picture of the superposition of* H. pylori *holoflavodoxin (orange) and apoflavodoxin (green) main chains structures. FMN is represented in sticks and coloured by atom type while the chloride ion is shown as a green sphere. The benzamidine additive of the apoflavodoxin structure is represented in sticks, and it is coloured in blue. Superposition of residues located at the FMN binding site of* H. pylori *holoflavodoxin (orange) and apoflavodoxin (green). FMN is coloured by atom type and the chloride ion is represented as a green sphere. Several water molecules found in the apoflavodoxin structure are shown in red. [Color figure can be viewed in the online issue, which is available at www.interscience.wiley.com.]*

mimicking the O4 atom of FMN in the holo protein, appears bonded to the O atom of Gly56 (2.64 Å) and to the N atom of Gly58 (2.82 Å). In the holo protein, the O4 atom is bound to the N atom of Gly58 (3.27 Å) and to the O atom of Ala55 (2.98 Å). The water molecule mimicking O2 makes hydrogen bonds with the N atoms of Asp88 and Ala97, exactly like the O2 atom in the holoprotein. The water mimicking the N10 atom forms a hydrogen bond with the N and O atoms of Gly56, helping to anchor this residue in its new conformation in the apo form.

Another region implicated in FMN binding in the holoprotein involves the 9–13 loop together with the N-terminus of helix 1 (spanning residues 14–26). More specifically, the interaction takes place between the Thr10-Ala15 segment and the FMN phosphate. Mutational studies in the *Anabaena* complex have shown that this interaction is the major contributor to the stability of the complex.[9]

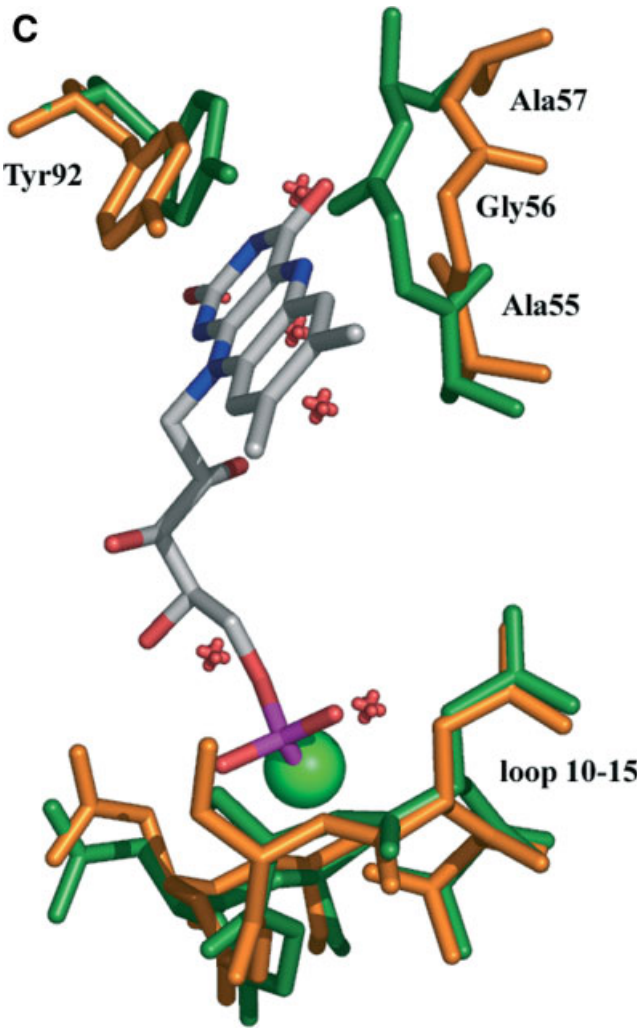

Figure 1
(Continued)

Somewhat surprisingly, the rms deviation of all backbone atoms in this region between the holo and apo structures is of just 0.51 Å, similar to the overall one [Fig. 1(B)]. A strong density peak in apoflavodoxin appeared at the site where the phosphate group of FMN is located in the holoflavodoxin structure. This globular density was compatible with a chloride anion, present in the crystallization medium, while refinement trials using a water molecule as model failed. The ion is at hydrogen bonding distances (Table II) of the OG of Thr10 and Ser 12, the N of Ala15 and two solvent molecules. Table II shows how the interactions established by the FMN phosphate group in holoflavodoxin have been replaced by equivalent or new ones formed by the chloride ion in apoflavodoxin. The side chain of Ser12 that is bound to the O1P atom of FMN in the holo structure changes its conformation to form a new hydrogen bond with the chloride ion. The Thr10 side chain is also bound to the ion, and the N atom of Ala15 is close enough to form an additional H-bond. However, Asp11, that appeared H-bonded to the FMN phosphate, establishes an H-bond with the side chain of Thr10, and Gly13 and Asn14 replace their interactions with OP1 of FMN by new interactions with the side chain of Ser12. The interaction of the chloride ion with *Helicobacter pylori* apoflavodoxin resembles those described in the CLC chloride channel from *S. Typhimurium* and from *E. coli*,[48] with chloride ions bound to N termini of α-helices where the helix dipole provides a favourable electrostatic environment for anion binding.[49,50] It has been postulated[48] that the absence of a full positive charge prevents the ion from binding too tightly to chloride channels and therefore permits rapid ionic diffusion rates. In *H. pylori* apoflavodoxin, the chloride ion present in the crystallisation solution binds in a similar way near the N-terminus of helix α1 and it is thus possible that the binding is also not too tight.

As for the interaction between the FMN ribityl and the apoprotein, a mutational study performed on the *Anabaena* complex has shown that the ribityl hardly contributes to the affinity (9). In the *H. pylori* flavodoxin, the ribityl O3* atom is bound to Asp142 and the O4* to Asn14. In the apoprotein, both Asp142 and Asn14 bind water molecules. The overall change in apoflavodoxin upon cofactor binding is displayed in Figure 2. Whereas the polypeptide conformation in the holoflavodoxin shows a cavity that is perfectly shaped to accommodate the bound FMN cofactor, in apoflavodoxin the isoalloxazine site is partly filled by the approximation of the isoalloxazine binding loops, while the phosphate binding site, although in a native conformation, is also filled by a bound chloride ion. Finally, at the region were a benzamidine molecule appears bound in apoflavodoxin, there are three interacting residues. The OE2 atom of Glu30 is bound to the N2 atom of benzamidine (2.95 Å) and to the N atom of Gly2 (3.00 Å). The aromatic ring of Phe45 is at 3.77 Å to that of benzamidine allowing for a stacking interaction. The apo and holo structures show for these three residues an r.m.s. deviation of 0.73 Å.

Structural comparison between the *H. pylori* and *Anabaena* apoflavodoxins

The only apoflavodoxin structure available until now was that of *Anabaena* PCC 7119.[26] A superposition of the structures of the *Anabaena* and *H. pylori* apoflavodoxins shows that both are quite similar (rmsd 1.04 Å). In the isoalloxazine binding site of *Anabaena* apoflavodoxin,[28] large changes in dihedral angles relative to those in the holoprotein allow the side chain of Trp57 (equivalent to Ala55 in *H. pylori* flavodoxin) to penetrate into the depression previously occupied by the pyrimidine portion of the isoalloxazine (Fig. 2) where it contacts Tyr94 (which moves towards the Trp) establishing a stacking interaction that leaves the two aromatic residues

DOI 10.1002/prot

Table II
Intramolecular Interactions Involving Residues in FMN Phosphate and Ribityl Binding Sites in H. pylori and Anabaena *PCC 7119 Flavodoxin Structures*

	Helicobacter pylori					*Anabaena* PCC 7119	
	Apoflavodoxin		Holoflavodoxin[a]			Apoflavodoxin[b]	
	Hydrogen bonds		Hydrogen bonds			Hydrogen bonds	
Residue	Partner	Distance (Å)	Partner	Distance (Å)	Residue	Partner	Distance (Å)
Thr10 (OG1)	Cl^-	2.83	FMN (O3P)	2.43	Thr10 (OG1)	SO_4 (O1)	2.8
Asp11(N)	Thr10(OG1)	3.18	FMN (O2P)	3.04	Gln11 (N)	SO_4 (O4)	2.9
	H_2O	2.72					
Ser12 (OG)	Cl^-	3.18	FMN (O1P)	3.19	Thr12 (OG1)	SO_4 (O2)	2.7
Ser12 (N)	H_2O	3.16	FMN (O2P)	3.13	Thr12 (N)	SO_4 (O2)	3.2
						SO_4 (O4)	3.1
Gly13 (N)	Ser12 (OG)	3.16	FMN (O1P)	3.32	Gly13		
Asn14 (N)	Ser12 (OG)	3.17	FMN (O1P)	3.24	Lys14 (N)	SO_4 (O2)	2.8
Asn14 (OD1)	H_2O	2.98	FMN (O1P)	3.28			
			FMN (O4*)	3.14			
Ala15 (N)	Cl^-	3.25	FMN (O3P)	2.88	Thr15 (N)	SO_4 (O1)	2.8
Asp142 (OD2)			FMN (O3*)	2.43			
			H_2O	2.65			
Asp142 (OD1)	H_2O	2.98	FMN (O3*)	3.31	Asp146 (OD1)	Lys14 (NZ)	3.5

[a]Data from structure ((28); pdb: 1FUE).
[b]Data from 13.

at 3.8 Å. In *H. pylori* apoflavodoxin, Ala55 does not experience such a large conformational change. However, the neighboring Gly56 flips so that its carbonyl oxygen points towards the depression. This is accompanied by a concerted approaching movement of Tyr92 (Fig. 2), which brings its CZ to 3.23 Å of the Gly oxygen. In this way the entrance to the isoalloxazine site is closed. Although the stabilization in *H. pylori* apoflavodoxin of the empty FMN binding site is thus not reached by an aromatic–aromatic interaction as in *Anabaena*, the mechanism is nevertheless very similar as it involves extensive rearrangements of the 55–60 loop, which fills the site by interaction with an approaching Tyr side chain located in the other binding loop.

The residues of *Anabaena* apoflavodoxin interacting with the phosphate and ribityl moieties of FMN and those occupying similar structural positions in the apo protein from *H. pylori* are shown in Table II and Figure 3. All residues in the 10–15 region, with the exception of Gly13, are forming hydrogen bonds with the sulphate group in *Anabaena* apoflavodoxin. However, in the *H. pylori* apoprotein, neither Gly13 nor Asp11 and Asn14 make H-bonds with the chloride ion that replaces the missing FMN phosphate. On the other hand, whereas Lys14 in *Anabaena* apoflavodoxin is bound by its NZ to the OD1 of Asp146, no equivalent interaction between Asn14 and Asp142 is observed in *H. pylori* apoflavodoxin.

H. pylori flavodoxin as a drug target: Binding of small charged molecules in the pocket near FMN

Flavodoxin is an essential protein for the survival of *H. pylori*.[19] A recent study aimed at identifying inhibitors of the protein[20] has shown that a small organic molecule, benzylamine, is able to bind the holoprotein in the pocket near FMN that appears as a consequence of the lack of a Trp residue in the 55–60 loop. Since the crystallization buffer of *H. pylori* apoflavodoxin contains benzamidine as an additive, which is quite similar to benzylamine, there was a chance that the additive appeared bound at the pocket near the empty FMN binding site. However, no electron density that could be assigned to the presence of benzamidine near the pocket was observed. Instead, one molecule of benzamidine was located near the N-terminus of the protein, far away from the FMN binding site; Figure 1(A). This fact could be related with the partly closed conformation of the FMN binding pocket, however careful inspection of the molecular surfaces of the holo and apo forms (Fig. 2) suggests that the pocket itself is still present in apoflavodoxin. Alternatively, the presence of FMN could be required for benzamidine binding if the complex were stabilised by cation-π interactions[51–53] with the isoalloxazine moiety of FMN. To determine whether benzamidine can actually bind holoflavodoxin at the FMN neighbouring pocket, a spectroscopic titration of FMN fluorescence has been performed. Indeed, the charged benzamidine binds to holoflavodoxin markedly quenching FMN fluorescence (Fig. 3), and the dissociation constant of the holoflavodoxin-benzamidine complex at 25°C is calculated at 10 m*M*, which is the same value, within error, as that reported for the benzylamine complex.[20] It seems thus that the binding of small charged molecules at the pocket near FMN is favored by the presence of the cofactor.

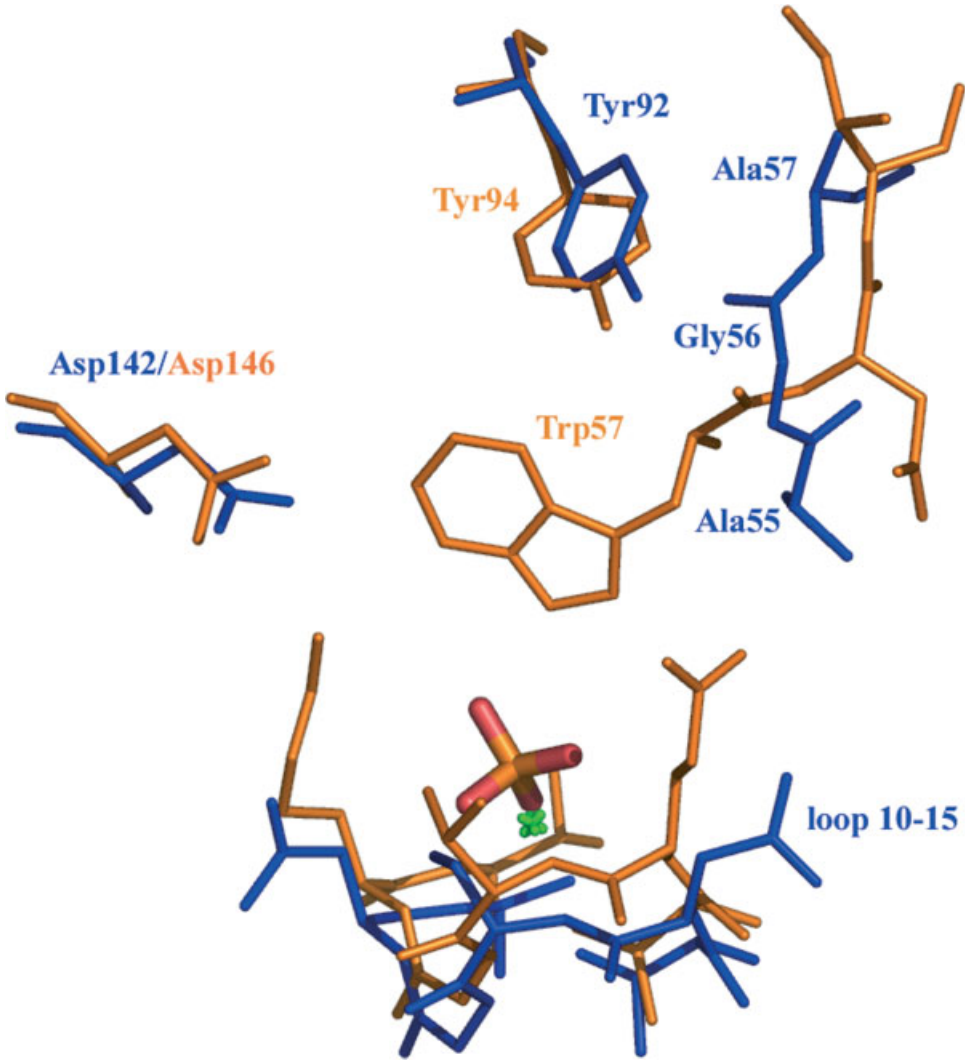

Figure 2

Comparison of the FMN binding sites of Anabaena *(orange) and* H. pylori *(blue) apoflavodoxins. In the* Anabaena *apoflavodoxin the isoalloxazine site is closed by the approximation of the Trp57 side chain to Tyr94 (which is facilitated by a conformational change in the Trp57 loop). In* H. pylori *apoflavodoxin the isoalloxazine site is closed by a similar conformational change, but Tyr92 simply contacts main chain atoms of a glycine residue (Gly56). While in the* Anabaena *structure the FMN phosphate binding site display a bound sulphate (or phosphate) anion from the crystallization buffer (coloured by atom type), in the* H. pylori *one there is a bound chloride anion (shown in green). In both cases the conformation of the FMN phosphate site is native-like. The FMN binding site is thus closed at the isoalloxazine site and bears an anion at the phosphate site. [Color figure can be viewed in the online issue, which is available at www.interscience.wiley.com.]*

Normal mode and principal component analyses of apoflavodoxin motions

NMA of minimized structures provides useful information on the mobility and correlation between different protein regions, and it seems worthwhile to apply this method to gain insight in the mechanism of FMN binding. The results of all-atom calculations for the lowest frequency mode are compared in Figure 4 with those of the GNM approximation (see Methods). When only C_α displacements are plotted, an agreement between the two methods is clear, which validates the coarse-grained approach. Several regions appear to be more flexible in the collective motion. The maximum amplitude of the mode corresponds to loop 55–60. This movement is correlated with the region of Tyr92 (loop 88–98) that corresponds to the second amplitude peak. The two isoalloxazine binding loops are thus the two more flexible regions of the apoprotein. Additional large amplitudes of the mode correspond to regions adjacent to the binding loops, that is: residues 120–130 (matching the loop spe-

DOI 10.1002/prot

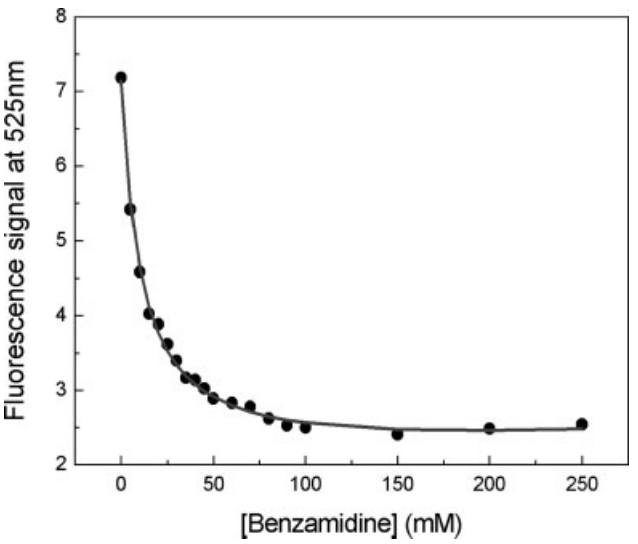

Figure 3

Binding of benzamidine to H. pylori *holoflavodoxin. The quenching of FMN fluorescence associated to the binding of benzamidine has been used to calculate the strength of the complex. According to the X-ray structure, benzamidine does not bind at the pocket near the FMN binding site that is present in the apo form of* H. pylori *flavodoxin. The binding to holoflavodoxin is however clear and could be stabilized by cation/pi interactions with FMN.*

cific of long-chain flavodoxins, which has been described to experience at moderate temperatures pronounced structural changes leading to a thermal intermediate in the apoflavodoxin from *Anabaena*[16]) and a reverse turn, residues 34–37, adjacent to the 55–60 loop.

To gather information on the conformational fluctuations experienced by apoflavodoxin residues at different temperatures, molecular dynamics simulations have been performed. PCA is here especially interesting due to its ability to separate large concerted structural rearrangements from irrelevant fluctuations. We have focused on the two first principal components (Fig. 5). Thus, MD trajectories have been analyzed for several temperatures ranging from 50 to 330 K, with and without chloride ion in the binding site (see M&M section). The simulations reveal the arising, as the temperature increases, of coupled low frequency modes in regions that contribute to FMN binding (loops 55–60, 88–98). They are already present at 200 K and 300 K (not shown) and become more pronounced at 310 K, close to physiological temperatures. Interestingly, the coupling disappears at 330 K (not shown), which is probably related with the appearance at this temperature of a thermal unfolding intermediate of similar structure to that reported for the *Anabaena* apoflavodoxin thermal intermediate,[16] in which the two binding loops and the loop specific of long-chain flavodoxins are disorganized. This raises a note of caution with respect to the fairly common practice of performing simulations at high temperature in order to speed-up dynamics.[54] Our results suggest that great care is needed when performing flavodoxin simulations aiming at detecting possible variations in mobility, because thermal unfolding intermediates appear in all apoflavodoxins so far studied.[55]

In the absence of chloride at the FMN phosphate site, the PCA shows (see Fig. 5) a similar behaviour to that detected in NMA, that is: most of the mobility is concentrated in the isoalloxazine binding loops (residues 55–60 and 88–98) plus the long-chain flavodoxins specific loop, suggesting that moderate temperature fluctuations can induce conformational rearrangement (opening-closing) in the binding site. The presence of a chloride ion at the phosphate site (as mimicked by the inclusion of rigidity in the 9–13 loop) clearly reduces the contribution of the 55–60 loop to both PC eigenvectors. In contrast, loop 88–98 becomes more mobile (Fig. 5). It seems, thus, that the presence of a chloride ion bound at the FMN phosphate site (or possibly other anions, such as phosphate, in physiological conditions) exerts a profound effect on the mobility of the two isoalloxazine loops.

Recently, MD simulations of the influence of phosphate in the dynamics of the flavodoxin from D. *desulfuricans* have been reported.[54] These authors use as initial conditions of their simulations the structure of the holoflavodoxin after *in silico* removal of the FMN group,

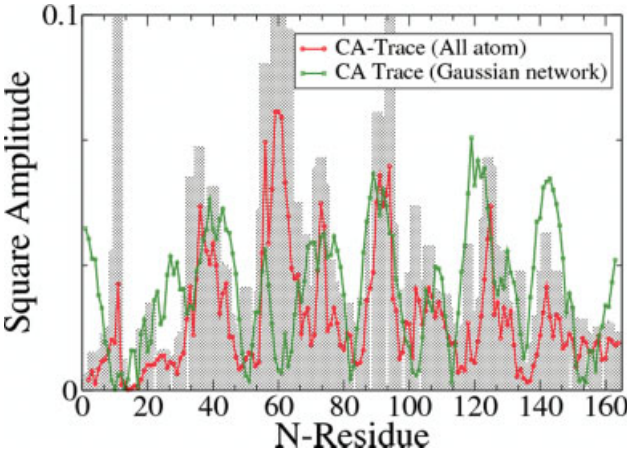

Figure 4

Square amplitude of the lowest normal mode of the apoflavodoxin from H. pylori. *The contribution of the Cα atoms to the lowest mode of the minimized structure (all-atoms simulation with the CHARMM force field) is shown in red. The green line comes from a coarse-grained approach (see M&M) and represents the square amplitude of the first normal mode of the GNM analysis. In grey shadow, the all atom average amplitude per residue is shown. The good agreement between the Gaussian Network's mode and the corresponding amplitudes arising from the all-atom analysis underlines the relevance of the correlated motions of the 55-60 and 88-98 loops, as well as the usefulness of the simplified model. [Color figure can be viewed in the online issue, which is available at www.interscience.wiley.com.]*

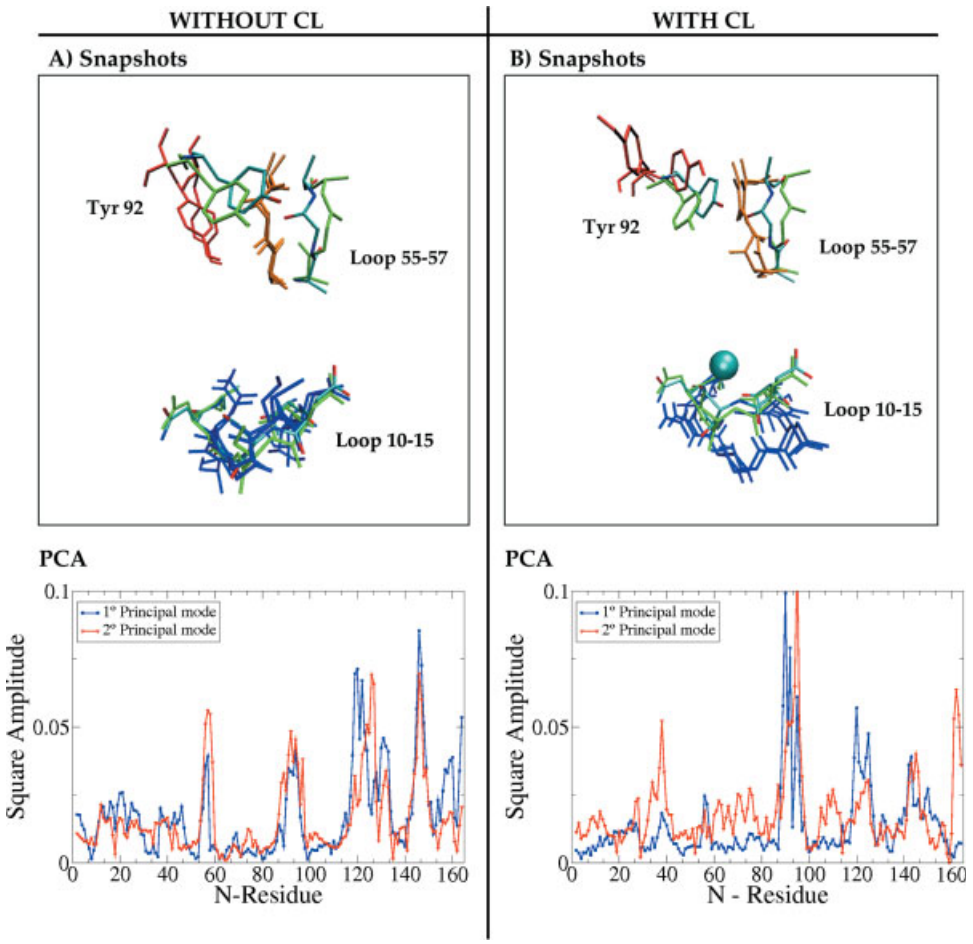

Figure 5

*Summary of the MD analysis discussing the effect of the anion presence at the binding site. (***Top panels***): Superposition of two representative snapshots of residues taking part of the FMN binding site extracted from trajectories at 310K. The holo structure (green) and the apo structure (light blue) are also represented. (***Bottom panels***): Graphical comparisons of the first and second principal modes (PCA) describing the magnitude of fluctuations per residue without chloride (***A***) and with chloride ion (***B***). The colour lines correspond to the Cα contributions to the principal mode at T=310 K. In the presence of chloride, the cooperative large amplitude motion observed between the isoalloxazine binding loops 55-60 and 88-98 disappears, the mobility of loop 55-57 is decreased, and that of loop 88-98 is enhanced. [Color figure can be viewed in the online issue, which is available at www.interscience.wiley.com.]*

because the structure of the corresponding apo form is not available. Thus, their trajectories may well capture some relaxations events not related to anion binding. In addition, the simulations are performed at a high temperature where the native state is not the dominant conformation (see above). In spite of these differences, the two studies support that binding of either phosphate (in *D. desulfuricans*) or chloride (in *H. pylori*) induces a higher rigidity in the 50–55 binding loop. Whether this facilitates the binding of the cofactor remains, in our view, uncertain. However, it is possible that the greater mobility (and accessibility) of Tyr92 in the presence of a bound anion may assist in the binding reaction where this tyrosine is expected to be crucial, as judged from the role of the equivalent tyrosine residues in the apoflavodoxins from other species.[10,54]

Insight into the mechanism of FMN binding by apoflavodoxin

The FMN molecule consists of three parts: the redox active isoalloxazine ring, the connecting ribityl chain, and the terminal phosphate. Both the isoalloxazine and the phosphate binding sites are more conserved among flavodoxins than the ribityl one.[28] Thermodynamic analysis of the contribution of each of these parts to the binding energy of the complex indicates that the phosphate and the ring make the greatest contributions, while the ribityl

DOI 10.1002/prot

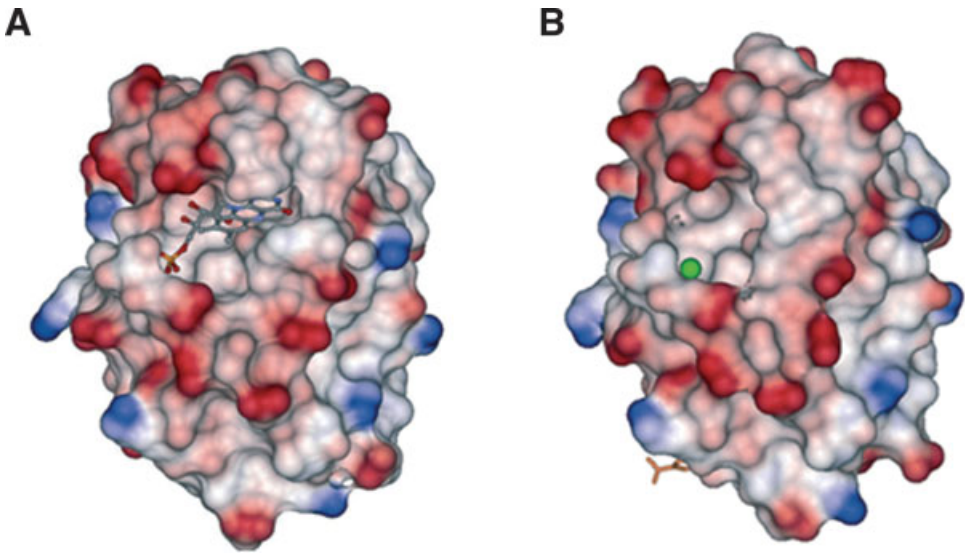

Figure 6

*(**A**) Molecular surface representation of the holo* H. pylori *flavodoxin showing the electrostatic potential (negative in red and positive in blue). The FMN cofactor is drawn in a stick representation. (**B**) Molecular surface representation of the apo* H. pylori *flavodoxin. A chloride ion is represented as a green sphere. A large part of the FMN binding pocket of the holoprotein appears closed in the apo structure. In contrast, the phosphate biding site is in a nativelike conformation and bears a chloride ion. [Color figure can be viewed in the online issue, which is available at www.interscience.wiley.com.]*

hardly stabilises the complex.[9] One would thus expect that the apoflavodoxin/FMN primary recognition event took place at either the phosphate or the isoalloxazine site. The structure of the apoflavodoxin from *Anabaena* revealed that the isoalloxazine pocket was closed while the phosphate binding site appeared in a native conformation with a bound sulphate ion from the crystallisation buffer perfectly mimicking the conformation of the FMN phosphate in the holoprotein. Based in this structure, it seemed to us plausible that FMN binding would start by interaction at the phosphate site, which would either trigger the opening of the isoalloxazine site or simply increase the rate of isoalloxazine intercalation between Trp57 and Tyr94 by a proximity effect. Subsequent mutational and kinetic work in our laboratory on the *Anabaena* complex, however, evidenced[10] that the transition state of binding involved strong and weak, respectively, interactions between the isoalloxazine and the side chains of Tyr94 and Trp57, and no interactions with the phosphate binding residues Thr12 and Thr15, which strongly suggests that the primary recognition event takes place at the isoalloxazine site. This is also supported by the fact that riboflavin (nonphosphorilated FMN) binds much faster to apoflavodoxin than FMN.[10] An important energetic role of the aromatic residues at the isoalloxazine site in the transition state of binding has also been recently observed in other flavodoxin,[54] while other studies have stressed the possibility of alternative primary binding events taking place at the phosphate or at the isoalloxazine site depending on the concentration of phosphate in the solution.[56–58]

We have now determined the X-ray structure of a second apoflavodoxin, from the pathogen *Helicobacter pylori,* avoiding both high ionic strength conditions and the presence of phosphate or sulphate ions. Comparison of the structures of the *Anabaena* and *Helicobacter* apoflavodoxins allows discerning whether the distinctive features observed in the *Anabaena* X-ray structure are due to the buffer conditions or just characteristic of the protein. In spite of not having a bulky Trp side chain in the 55–60 binding loop that could help to stabilise an alternative loop conformation by forming an interaction with Tyr92, large rearrangements of the dihedral angles of several residues in the *Helicobacter* 55–60 loop allow it, nevertheless, to approach Ty92 and close the empty isoalloxazine site (Fig. 6). The interaction between the two loops is reinforced in the *Helicobacter* apoprotein by new contacts established between the Gly56 carbonyl oxygen and the CZ atom of Tyr92 (at 3.23 Å in the apoprotein but quite distant in the functional complex: 8.20 Å) and by the Gly58 CA carbon and the side chain oxygen of Thr95 (3.46 Å in the apoprotein and 4.79 Å in the complex). Thus, the isoalloxazine binding site appears also closed in the *Helicobacter* apoprotein and the closure can not be attributed either to strong interactions between aromatic binding residues or to a strengthening of hydrophobic interactions in high ionic strength conditions. It

seems that the 55–60 loop displays significant structural flexibility (previously noticed in X-ray studies of wild type and mutant *Anabaena* variants[9]), which allows it, in the apo form, to fill the empty space left by the cofactor and give rise to a more compact and more stable conformation. Although the temperature factors of the isoalloxazine binding sites in the two apoflavodoxins are not especially high, it should be recalled that the NMR evidence on the *Anabaena* and *Azotobacter* apoflavodoxins[26,27] seems to indicate that the closed, more stable structures observed in the crystal, are probably in equilibrium with more open conformations. We have investigated the flexibility of these binding loops by NMA and PCA using both simplified and all-atom simulations, and our analysis indicates that these loops are, together with the long loop specific of long-chain flavodoxins, the most flexible regions of the protein, and that their dynamics are coupled and markedly influenced by the presence of anions bound at the phosphate site. Besides, the simulations capture the expected uncoupling of these three loops at around 330 K, where the *Anabaena* apoflavodoxin has been described to populate an alternative partly unfolded conformation in which the three loops are disorganized.[16]

The additional focus of interest relating the mechanism of FMN recognition is the phosphate binding site. This time, neither phosphate nor sulphate ions were present in the crystallization buffer, yet *Helicobacter* apoflavodoxin unexpectedly managed to bind a chloride ion that similarly mimics the FMN phosphate of the holoprotein. Since the chloride concentration in the buffer was not very high (0.2 *M*) we interpret that, in the absence of the cofactor, the phosphate binding loop and N-terminus of helix 1 capture other suitable small anions available in the solution. This raises a note of caution for the future design and interpretation of kinetic studies of FMN/apoflavodoxin interaction as a function of phosphate. As they have often been done at constant, high ionic strength values, typically provided by high sodium chloride concentrations[10,57] it is quite possible that chloride ions were bound in the phosphate binding site at low phosphate concentrations. Having or not having phosphate in the solution might not be as important in this respect as having a high or a low concentration of small anions.

CONCLUSIONS

The two apoflavodoxin structures (1ftg[28] and 2bmv, this work) thus tell us that, in spite of differences in sequence and in crystallisation conditions, apoflavodoxins (at least long-chain ones) display closed, non-native, isoalloxazine binding sites together with native-like, rather promiscuous, phosphate binding sites that tend to carry bound anions. In this respect, neither of the two binding hot spots in apoflavodoxins is readily available for FMN interaction: the isoalloxazine site due to its closed conformation and the phosphate site due to the presence of alternative ions. The mutational analysis of the transition state of binding, and the faster binding of riboflavin compared to FMN[10] suggest that the recognition begins at the isoalloxazine site, which could be facilitated by the well-documented flexibility of the isoalloxazine binding loops by X-ray,[9] by NMR[26,27] and by computer simulations (this work). Since it now appears that apoflavodoxins, under physiological conditions, will generally bear bound anions at the binding site of the FMN phosphate, the proposed role of such anions (whether phosphate or others) in facilitating the opening of the isoalloxazine site cannot be discarded at present. In this respect, our simulations suggest that ion binding could make the Trp and Tyr loops less and more mobile, respectively. Whether this contributes to facilitate FMN binding remains to be tested.

ACKNOWLEDGMENTS

NC, MB, SC and DP were supported by MEC fellowships, CM by a fellowship from the Junta de Andalucía (Spain) and IP-D by a CSIC fellowship.

REFERENCES

1. Mayhew SG, Tollin G. General properties of flavodoxins. In: Müller F, editor. Chemistry and biochemistry of flavoenzymes, Vol. III. Boca Raton, Florida: CRC Press; 1992. pp 427–466
2. Ludwig ML, Luschinsky CL. Structure and redox properties of *Clostridial* flavodoxin. In: Müller F, editor. Chemistry and biochemistry of flavoenzymes, Vol III. Boca Raton, Florida: CRC Press; 1992. pp 427–466.
3. Sancho J. Flavodoxins: sequence, folding, binding, function and beyond. Cell Mol Life Sci 2006;63:855–864.
4. Andersen RD, Apgar PA, Burnett RM, Darling GD, Lequesne ME, Mayhew SG, Ludwig ML. Structure of the radical form of clostridial flavodoxin: a new molecular model. Proc Natl Sci USA 1972;69: 3189–3191.
5. Watenpaugh KD, Sieker LC, Jensen LH, Legall J, Dubourdieu M. Structure of the oxidized form of a flavodoxin at 2.5-Angstrom resolution: resolution of the phase ambiguity by anomalous scattering. Proc Natl Acad Sci USA 1972;69:3185–3188.
6. Gómez-Moreno C, Martínez-Júlvez M, Medina M, Hurley JK, Gordon T. Protein-protein interaction in electron transfer reactions: the ferredoxin/flavodoxin/ferredoxin:$NADP^+$ reductase system from *Anabaena*. Biochemie 1998;80:837–846.
7. Martínez-Júlvez M, Nogués I, Hurley JK, Tollin G, Medina M, Gómez-Moreno C. Molecular recognition between ferredoxin-$NADP^+$ reductase and its protein partners: role of charged and hydrophobic residues. Flavins and Flavoproteins Proceeding 13th Symposium; Berlin: 1999. pp 293–296.
8. Nogués I, Martínez-Júlvez M, Navarro JA, Hervás M, Armenteros L, de la Rosa MA, Brodie TB, Hurley JK, Tollin G, Gómez-Moreno C, and Medina M. Role of hydrophobic interactions in the flavodoxin mediated electron transfer from photosystem I to ferredoxin-$NADP^+$ reductase in *Anabaena PCC 7119*. Biochemistry 2003;42: 2036–2045.
9. Lostao A, El Harrous M, Daoudi F, Romero A, Parody-Morreale A, Sancho J. Dissecting the nergetics of the Apoflavodoxin-FMN Complex. J Biol Chem 2000;275:9518–9526.

 DOI 10.1002/prot

10. Lostao A, Daoudi F, Irun MP, Ramon A, Fernandez-Cabrera C, Romero A, Sancho J. How FMN binds to anabaena apoflavodoxin: a hydrophobic encounter at an open binding site. J Biol Chem 2003;278:24053–24061.
11. Fernández-Recio J, Genzor CG, Sancho J. Apoflavodoxin folding mechanism: an alpha/beta protein with an essentially off-pathway intermediate. Biochemistry 2001;40:15234–15245.
12. Bollen YJM, Sánchez IE, van Mierlo CP. Formation of on- and off-pathway intermediates in the folding kinetics of *Azotobacter vinelandii* apoflavodoxin. Biochemistry 2004;43:10475–10489.
13. Genzor CG, Beldarrain A, Gomez-Moreno C, Lopez-Lacomba JL, Cortijo M, Sancho J. Conformational stability of apoflavodoxin. Protein Sci 1996;5:1376–1388.
14. van Mierlo CP, van Dongen WMAM, Vergeldt F, van Berkel WJH, Steensma E. The equilibrium unfolding of *Azotobacter vinelandii* apoflavodoxin II occurs via a relatively stable folding intermediate. Protein Sci 1998;7:2331–2344.
15. Campos LA, Garcia-Mira MM, Godoy-Ruiz R, Sanchez-Ruiz JM, Sancho J. Do proteins always benefit from a stability increase? Relevant and residual stabilisation in a three-state protein by charge optimisation. J Mol Biol 2004;344:223–237.
16. Campos LA, Bueno M, Lopez-Llano J, Jiménez ,MA, Sancho J. Structure of stable protein folding intermediates by equilibrium phi-analysis: the apoflavodoxin thermal intermediate. J Mol Biol 2004;344:239–255.
17. Campos LA, Cuesta-López S, López-Llano J, Falo F, Sancho J. A double-deletion method to quantifying incremental binding energies in proteins from experiment: example of a destabilizing hydrogen bonding pair. Biophyscal J 2005;88:1311–1321.
18. Paul R, Bosch FU, Schafer KP. Overexpression and purification of Helicobacter pylori flavodoxin and induction of a specific antiserum in rabbits. Protein Expr Purif 2001;22:399–405.
19. Freigang J, Diederichs K, Schafer KP, Welte W, Paul R. Crystal structure of oxidized flavodoxin, an essential protein in *Helicobacter pylori*. Protein Sci 2002;11:253–261.
20. Cremades N, Bueno M, Toja M, Sancho J. Towards a new therapeutic target: *Helicobacter pylori* flavodoxin. Biophys Chem 2005;115: 267–276.
21. Smith WW, Pattridge KA, Ludwig ML, Petsko GA, Tsernoglou D, Tanaka M, Yasunobu KT. Structure of the oxidized flavodoxin from *Anacystis nidulans*. J Mol Biol 1983;165:737–755.
22. Fukuyama K, Wakabayashi S, Matsubara H, Rogers LJ. Tertiary structure of oxidized flavodoxin from an eukaryotic red alga *Chondrus crispus* at 2.35 Å resolution. J Biol Chem 1990;265:15804–15812.
23. Watt W, Tulinsky A, Swenson RP, Watenpaugh KD. Comparison of the crystal structures of a flavodoxin in its three oxidation states at cryogenic temperatures. J Mol Biol 1991;218:195–208.
24. Rao ST, Shaffie F, Yu C, Satyshur KA, Stockman BJ, Marley JL, Sundaralingam M. Structure of the oxidized long-chain flavodoxin from *Anabaena* 7120 at 2 Å resolution. Protein Sci 1992;1:1413–1427.
25. Ingelman M, Bianchi V, Eklund H. The three-dimensional structure of flavodoxin reductase from *Escherichia coli* at 1.7 Å resolution. J Mol Biol 1997;268:147–157.
26. Steensma E, van Mierlo CP. Structural characterisation of apoflavodoxin shows that the location of the stable nucleus differs among proteins with a flavodoxin-like topology. J Mol Biol 1998;282:653–666.
27. Langdon GM, Jimenez MA, Genzor CG, Maldonado S, Sancho J, Rico M. *Anabaena* apoflavodoxin hydrogen exchange: on the stable exchange core of the alpha/beta (21345) flavodoxin-like family. Proteins 2001;43:476–488.
28. Genzor C, Perales-Alcón A, Sancho J, Romero A. Closure of a tyrosine/tryptophan aromatic gate leads to a compact fold in apoflavodoxin. Nat Struct Biol 1996;3:329–332.
29. Edmondson DE, Tollin G. Chemical and physical characterization of the Shethna flavoprotein and apoprotein and kinetics and thermodynamics of flavin analog binding to the apoprotein. Biochemistry 1971;10:124–132.
30. Gill SC, von Hippel PH. Calculation of protein extinction coefficients from amino acid sequence data. Anal Biochem 1989;182:319–326.
31. Minor W, Steczko J, Stec B, Otwinowski Z, Bolin JT, Walter R, Axelrod B. Crystal structure of soybean lipoxygenase L-1 at 1.4 Å resolution. Biochemistry 1996;35:10687–10701.
32. Vagin A, Teplyakov A. MOLREP: an automated program for molecular replacement. J Appl Cryst 1997;30:1022–1025.
33. Murshudov CN, Vagin AA, Dodson EJ. Refinement of macromolecular structures by the maximum-likelihood method. Acta Crystallogr D Biol Crystallogr 1997;53:240–255.
34. Jones TA, Zou JY, Cowan SW, Kjeldgaard M. Improved methods for building protein models in electron density maps and the location of errors in these models. Acta Crystallogr Sect A 1991;47:110–119.
35. Go N, Noguti T, Nishikawa T. Dynamics of a small globular protein in terms of low-frequency vibrational modes. Proc Natl Acad Sci USA 1983;80:3696–3700.
36. Brooks BR, Karplus M. Harmonic dynamics of proteins: normal modes and fluctuations in bovine pancreatic trypsin inhibitor. Proc Natl Acad Sci USA 1983;80:6571–6575.
37. Brooks B, Bruccoleri R, Olafson B, States D, Swaminathan S, Karplus M. CHARMM: a program for macromolecular energy, minimization, and dynamics calculations. J Comp Chem 1983;4:187–217.
38. Tirion MM. Large amplitude elastic motions in proteins from a single-parameter, atomic analysis. Phys Rev Lett 1996;77:1905–1908.
39. Haliloglu T, Bahar I, Erman B. Gaussian dynamics of folded proteins. Phys Rev Lett 1997;79:3090–3093.
40. Demirel MC, Atilgan AR, Jernigan RL, Erman B, Bahar I. Identification of kinetically hot residues in proteins. Protein Sci 1998;7: 2522–2532.
41. Bahar I, Erman B, Jeringan RL, Atildan RA, Novell DG. Collective motions in HIV-1 reverse transcriptase: examination of flexibility and enzyme function. J Mol Biol 1999;285:1023–1037.
42. Delarue M, Sanejouand YH. Simplified normal mode analysis of conformational transitions in DNA-dependent polymerases: the elastic network model. J Mol Biol 2002;320:1011–1024.
43. Sanejouand YH. Domain swapping of CD4 upon dimerization. Proteins 2004;57:205–212.
44. Hayward S, Go N. Collective variable description of native protein dynamics. Annu Rev Phys Chem 1995;46:223–250.
45. Van Aalten DMF, De Groot BL, Findlay JBC, Berendsen HJC, Amadei A. A comparison of techniques for calculating protein essential dynamics. J Comput Chem 1997;18:169–181.
46. López-Llano J, Maldonado S, Bueno M, Lostao A, Jiménez MA, Lillo MP, Sancho J. The long and short flavodoxins. I. The role of the differentiating loop in apoflavodoxin structure and FMN binding. J Biol Chem 2004;279:47177–47183.
47. López-Llano J, Maldonado S, Jain S, Lostao A, Godoy-Ruiz R, Sanchez-Ruiz JM, Cortijo M, Fernández-Recio J, Sancho J. The long and short flavodoxins. II. The role of the differentiating loop in apoflavodoxin stability and folding mechanism. J Biol Chem 2004;279: 47184–47191.
48. Dutzler R, Campbell EB, Cadene M, Chait BT, MacKinnon R. X-ray structure of a CLC chloride channel at 3.0 Å reveals the molecular basis of anion selectivity. Nature 2002;415:287–294.
49. Nicholson H, Becktel WJ, Matthews BW. Enhanced protein thermostability from designed mutations that interact with alpha-helix dipoles. Nature 1988;336:651–656.
50. Sancho J, Serrano L, Fersht AR. Histidine residues at the N- and C-termini of alpha-helices: perturbed pKas and protein stability. Biochemistry 1992;31:2253–2258.
51. Fernandez-Recio J, Romero A, Sancho J. Energetics of a hydrogen bond (charged and neutral) and of a cation-pi interaction in apoflavodoxin. J Mol Biol 1999;290:319–330.
52. Fernandez-Recio J, Vazquez A, Civera C, Sevilla P, Sancho J. The tryptophan/histidine interaction in alpha-helices. J Mol Biol 1997;267:184–197.

53. Loewenthal R, Sancho J, Fersht AR. Histidine-aromatic interactions in barnase. Elevation of histidine pKa and contribution to protein stability. J Mol Biol 1992;224:759–770.
54. Muralidhara BK, Chen MMAJ, Wittung-Stafshede P. Effect of inorganic phosphate on FMN binding and loop flexibility in *desulfovibrio desulfuricans* Apo-flavodoxin. J Mol Biol 2005;349:87–97.
55. Campos LA, Sancho J. Native-specific stabilization of flavodoxin by the FMN cofactor: a structural and thermodynamical explanation. Proteins 2006;63:581–594.
56. Murray TA, Foster MP, Swenson RP. Mechanism of flavin mononucleotide cofactor binding to the *Desulfovibrio vulgaris* flavodoxin, Part 2. Evidence for cooperative conformational changes involving tryptophan 60 in the interaction between the phosphate- and ring-binding subsites. Biochemistry 2003;42:2317–2327.
57. Murray TA, Swenson RP. Mechanism of flavin mononucleotide cofactor binding to the Desulfovibrio vulgaris flavodoxin, Part 1. Kinetic evidence for cooperative effects associated with the binding of inorganic phosphate and the 5′-phosphate moiety of the cofactor. Biochemistry 2003;42:2307–2316.
58. Bollen YJ, Nabuurs SM, van Berkel WJ, van Mierlo CP. Last in, first out: the role of cofactor binding in flavodoxin folding. J Biol Chem 2005;280:7836–7844.
59. Lazaridis T, Karplus M. Effective energy function for proteins in solution. Proteins 1999;35:133–152.

 DOI 10.1002/prot